Acta Pharmacologica Sinica (2016) 37: 1401–1412
 1671-4083/16
www.nature.com/aps

Original Article

DL0410, a novel dual cholinesterase inhibitor, protects mouse brains against Aβ-induced neuronal damage via the Akt/JNK signaling pathway

Dan ZHOU[1], Wei ZHOU[1], Jun-ke SONG[1], Zhang-ying FENG[1], Ran-yao YANG[1], Song WU[1], Lin WANG[1], Ai-lin LIU[1, 2, *], Guan-hua DU[1, 2, *]

[1]State Key Laboratory of Bioactive Substance and Function of Natural Medicines, Institute of Materia Medica, Chinese Academy of Medical Sciences and Peking Union Medical College, Beijing 100050, China; [2]Beijing Key Laboratory of Drug Target and Screening Research, Beijing 100050, China

Aim: 1,1′-([1,1′-Biphenyl]-4,4′-diyl)*bis*(3-(piperidin-1-yl)propan-1-one)dihydrochloride (DL0410) is a novel synthetic dual acetylcholinesterase (AChE)/butyrocholinesterase (BuChE) inhibitor, which has shown a potential therapeutic effect on Alzheimer's disease (AD). In this study we examined whether DL0410 produced neuroprotective effects in an AD cellular model and an $A\beta_{1-42}$-induced amnesia mouse model.

Methods: The *in vitro* inhibitory activities against AChE and BuChE were estimated using Ellman's assay. Copper-induced toxicity in APPsw-SY5Y cells was used as AD cellular model, the cell viability was assessed using MTS assay, and cell apoptosis was evaluated based on mitochondrial membrane potential detection. $A\beta_{1-42}$-induced amnesia mouse model was made in male mice by injecting aggregated $A\beta_{1-42}$ (2 μg in 2 μL 0.1% DMSO) into the right cerebral ventricle. Before and after $A\beta_{1-42}$ injection, the mice were orally administered DL0410 (1, 3, 9 $mg \cdot kg^{-1} \cdot d^{-1}$) or rivastigmine (2 $mg \cdot kg^{-1} \cdot d^{-1}$) for 3 and 11 d, respectively. Memory impairments were examined using Morris water maze (MWM) test and passive avoidance test. The expression levels of APP, CREB, BDNF, JNK and Akt in the mouse brains were measured with either immunohistochemistry or Western blotting.

Results: DL0410 exhibited *in vitro* inhibitory abilities against AChE and BuChE with IC_{50} values of 0.286±0.004 and 3.962±0.099 μmol/L, respectively, which were comparable to those of donepezil and rivastigmine. In APPsw-SY5Y cells, pretreatment with DL0410 (1, 3, and 10 μmol/L) decreased the phosphorylation of JNK and increased the phosphorylation of Akt, markedly decreased copper-stimulated $A\beta_{1-42}$ production, reversed the loss of mitochondrial membrane potential, and dose-dependently increased the cell viability. In $A\beta_{1-42}$-treated mice, DL0410 administration significantly ameliorated learning and memory deficits in MWM test and passive avoidance test. Furthermore, DL0410 administration markedly decreased $A\beta_{1-40/42}$ deposits in mouse cerebral cortices, and significantly up-regulated neurotrophic CREB/BDNF. Meanwhile, Akt/JNK signaling pathway may play a key role in the neuroprotective effect of DL0410.

Conclusion: DL0410 ameliorates cognitive deficit and exerts neuronal protection in AD models, implicating this compound as a candidate drug for the prevention and therapy of AD.

Keywords: Alzheimer's disease; amyloid β-peptides; cholinesterase inhibitor; DL0410; learning and memory; CREB/BDNF; Akt/JNK; neuroprotection

Acta Pharmacologica Sinica (2016) 37: 1401–1412; doi: 10.1038/aps.2016.87; published online 8 Aug 2016

Introduction

Alzheimer's disease (AD) is a progressive neurodegenerative disorder commonly leading to dementia in the elderly, which accounts for 60%–80% of all cases. In the global aging trend, the number of people with AD will increase to more than 100 million worldwide by 2050[1]. Although there have been several efforts to clarify the causes of this disease and explore effective pharmacologic therapies, no treatment has demonstrated potency in slowing the progression of AD[2].

Extracellular acetylcholine (ACh) is a key structural element in functional neural networks[3, 4]. Acetylcholinesterase (AChE) and butyrylcholinesterase (BuChE) are two major forms of cholinesterases in the mammalian brain. AChE plays a dominant role in halting cholinergic neurotransmission, but the physiological function of BuChE is not completely under-

*To whom correspondence should be addressed.
E-mail liuailin@imm.ac.cn (Ai-lin LIU);
dugh@imm.ac.cn (Guan-hua DU)
Received 2016-03-10 Accepted 2016-05-17

stood[5]. However, in the AD brain, AChE activity decreases from mild to severe stages, and BuChE activity is unchanged or even increased. BuChE might replace AChE in hydrolyzing brain ACh during AD progression[6, 7].

To date, cholinesterase inhibitors have been used as a first-line symptomatic therapy for AD[3]. Recent studies have shown that AChE and BuChE participate in AD progression. AChE accelerates the assembly of Aβ into amyloid fibrils; the peripheral binding site of AChE might be involved in amyloid formation[8–10]. BuChE activity has been associated with β-amyloid plaques in a transgenic AD mouse model[11]. Preclinical studies have indicated that the dual cholinesterase inhibitor rivastigmine exhibits a neuroprotective effect in fetal rat primary cortical cultures[11,12]. It is possible to identify a dual cholinesterase inhibitor that inhibits the activity of AChE and BuChE and simultaneously induces a neuroprotective effect.

The β amyloid peptide (Aβ) is a major component of extracellular senile plaques, which is a characteristic hallmark of AD[13]. Several studies have suggested that the $A\beta_{1-42}$ fragment is highly cytotoxic to neurons; this fragment has been widely used in *in vivo* and *in vitro* research to induce memory impairment and neuron damage[14–16]. Aβ causes mitochondrial dysfunction in neurons, leading to energy supplement impairment and mitochondria-mediated apoptosis[17, 18]. Numerous signaling pathways are involved in Aβ-induced neurotoxicity, including Wnt signal transduction pathways, the PI3K/Akt/mTOR pathway, the AMP-active protein kinase pathway and the sirtuin pathway [19–23].

DL0410 ((1,1′-([1,1′-biphenyl]-4,4′-diyl)*bis*(3-(piperidin-1-yl) propan-1-one)dihydrochloride, Figure 1), an acetylcholinesterase/butyrocholinesterase inhibitor, is a new synthetic compound belonging to phthalazinone units, which exhibits a different chemical structure among cholinesterase inhibitors, such as rivastigmine, donepezil, and tacrine. DL0410 was selected from more than 100 000 compounds using high-throughput screening assays for AChE and BuChE inhibitors. In a previous study, we showed that DL0410 binds to the active site of AChE, similar to donepezil, and the safety and efficacy of this compound were also confirmed using a series of experiments[24]. It has also been demonstrated that DL0410 improves cognitive deficits and reverses the plaque load in APP/PS1 transgenic mice[25]. In the present study, an $A\beta_{1-42}$-induced amnesia mouse model and an AD cellular model were used to investigate the protective effects and to explore the neuroprotective mechanisms of DL0410.

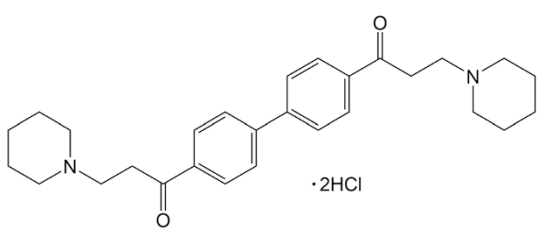

Figure 1. The structure of the candidate drug DL0410.

Materials and methods

Reagents

DL0410 (chemical purity was higher than 99% based on HPLC) was obtained from the National Center for Pharmaceutical Screening, Institute of Materia Medica, Chinese Academy of Medical Sciences (Bejing, China). Donepezil hydrochloride was purchased from the Jinan Chenghui Shuangda Chemical Industry Limited Company (Shandong, China). Rivastigmine was purchased from the Nantong Baihua Bio-pharmaceutical Company (Jiangsu, China). Hoechst 33342, acetylthiocholine iodide (ASCh), S-butyrylthiocholine chloride (BuSCh), tetraisopropyl pyrophosphoramide (iso-OMPA), and 5,5′-dithiobis(2-nitrobenzoic acid) (DTNB) were purchased from Sigma-Aldrich (St Louis, USA). A CellTiter 96®AQ_{ueous} One Solution Cell Proliferation Assay kit was purchased from Promega (Madison WI, USA). Rhodamine 123 (Rh123) was purchased from Dojindo Laboratory (Kumamoto, Japan). An Alexa Fluor 488-conjugated secondary antibody was purchased from Invitrogen (CA, USA).

The $A\beta_{1-42}$ peptide was purchased from Sangon Biotech (Shanghai, China) and dissolved in sterile 0.1% DMSO at a concentration of 1 mg/mL, followed by aggregation through incubation at 37 °C for 7 d prior to use. A human $A\beta_{1-42}$ ELISA Kit was purchased from Shanghai ExCell Biology, Inc. Human plasma was purchased from the Beijing Red Cross Blood Center. Primary antibodies against GAPDH, N-terminal kinase (JNK), and p-JNK were purchased from Cell Signaling Technology (Danvers, MA, USA). Primary antibodies against brain-derived neurotrophic factor (BDNF), p-Akt, cAMP-responsive element binding protein (CREB) and p-CREB were purchased from Epitomics (Burlingame, CA, USA). The anti-amyloid-β precursor protein (β-APP) antibody [Y188] (ab32136) was purchased from Abcam (Cambridge, UK). Anti-$A\beta_{1-40/42}$ (AB5076) was purchased from Millipore (MA, USA). An anti-rabbit IgG HRP-linked antibody (#7074) and an anti-mouse IgG HRP-linked antibody (#7076) were purchased from CST (Danvers, MA, USA).

An AChE inhibitory activity assay

Cholinesterase inhibitory activity was measured using Ellman's method with slight modifications[26]. The principle of this assay is that AChE hydrolyzes ASCh and generates choline iodide. Choline iodide reacts with DTNB as a thiol chromogenic agent to produce a yellow compound called TNB, which can be quantitatively measured through colorimetry. The quantity of choline iodide indicates the response to AChE activity.

AChE was extracted from rat brains, and the cerebral blood vessels were removed. Subsequently, 0.9% saline solution (20 mg/mL) was added, followed by centrifugation at 800×*g* for 10 min at 4 °C. The resulting supernatant was collected and used in an AChE inhibitory activity assay. Five serial dilutions of the samples were measured to inhibit AChE activity. In the AChE reaction system, the assay is performed in 96-well plates using 0.05 mol/L phosphate-buffered saline (PBS) and a Spectra Max M5 microplate reader (Molecular Devices, Sunny-

vale, CA, USA). The reaction system comprised 10 μL of test compounds, 30 μL of 0.05 mol/L PBS, 20 μL of AChE, 60 μL of 3.75 mmol/L ASCh, and 80 μL of 0.25 mg/mL DTNB. After a 60-min incubation at 37 °C, the absorbance intensity of the system was measured at 412 nm. Donepezil and rivastigmine were used as reference compounds.

A BuChE inhibitory activity assay

The experimental principle of this assay is similar to the assay above, where BuChE hydrolyzes BuSCh and generates choline iodide, which reacts with DTNB to produce TNB. TNB can be quantitatively measured through colorimetry. The quantity of choline iodide is indicated as the response to BuChE activity.

In this assay, BuChE was derived from human plasma and diluted 200 times in 0.05 mol/L PBS. The assay was performed in 96-well plates using a Spectra Max M5 microplate reader. The reaction system comprised 10 μL of test compounds, 40 μL of BuChE, 70 μL of 7.5 mmol/L BuSCh and 80 μL of 0.25 mg/mL DTNB. After incubation at 37 °C for 60 min, the absorbance intensity of the system was quantified at a wavelength of 412 nm. Rivastigmine and iso-OMPA were used as reference compounds.

Animals and treatments

Male ICR mice (18–22 g, Vital River Co, Beijing, China) were housed 4–5 per cage with free access to food and water under a 12/12 h day/night cycle. All experimental procedures in the present study were performed in accordance with institutional guidelines and ethics, and approval was obtained through the Laboratories Institutional Animal Care and Use Committee of the Chinese Academy of Medical Sciences and Peking Union Medical College.

The mice were randomized into six groups: sham group, $A\beta_{1-42}$-treated group, rivastigmine 2 mg/kg group[27], DL0410 1 mg/kg group, DL0410 3 mg/kg group, and DL0410 9 mg/kg group. Rivastigmine and DL0410 were dissolved in distilled water and administered to the mice through oral gavage once daily for 3 d, followed by injection with $A\beta_{1-42}$. After receiving the $A\beta_{1-42}$ injection, the mice were continuously treated with DL0410 or rivastigmine for 11 d.

Chloral hydrate powder was dissolved in 0.9% saline (1 g in 10 mL solution), and each mouse was anesthetized with an intraperitoneal (ip) injection at a dose of 400 mg/kg of body weight and placed on a stereotaxic frame. Aggregated $A\beta_{1-42}$ was implanted into the right cerebral ventricle according to the following coordinates: DV=-2.3 mm, ML=-1.0 mm and AP=0.4 mm caudal to bregma (2 μg in 2 μL 0.1% DMSO for each injection). The sham-operated animals were injected with the same amount of 0.1% DMSO in an identical manner.

Morris water maze test

Three days after receiving the $A\beta_{1-42}$ injection, the Morris water maze test was performed as previously described[28]. The experimental apparatus comprised a circular water tank (100 cm diameter, 35 cm height) containing water at 23±1 °C. A platform of 4.5 cm in diameter was placed at the midpoint of one quadrant (1 cm below the water surface). Each mouse received two training periods per day for five consecutive days. The latency and swim distance to escape from the water maze (finding the submerged escape platform) were calculated for each trial. In the probe trial, we recorded the number of times that the mice crossed the quadrant in the platform. All data were recorded using a computerized video system.

Passive avoidance test

The passive avoidance task was initiated 9 d after the $A\beta_{1-42}$ injection. The passive avoidance apparatus comprised an illuminated chamber attached to a darkened chamber containing a metal floor to deliver a mild electric shock[29]. A guillotine door separated the two compartments. The mice were placed into the illuminated chamber, facing away from the door of the dark chamber, and acclimated for 1 min. As soon as the mouse entered the dark chamber, the door was slid back into place, triggering an electric shock. The latency and error scores (the duration of time and number of times needed to enter the darkened chamber) were recorded. The retention test was conducted at 24 h later, placing the mouse in the illuminated chamber and using the same protocol but without the electric shock. The upper time limit was set at 300 s.

Immunohistochemistry analysis

After the behavioral experiments, the mice were anesthetized through an intraperitoneal (ip) injection of 10% chloral hydrate (0.04 mL/10 g), followed by transcardial perfusion with 50 mL of saline solution and 50 mL of 4% paraformaldehyde[30]. The brains were removed and fixed in 0.05 mol/L phosphate buffer (pH 7.4) containing 4% paraformaldehyde overnight. Each tissue block was embedded in paraffin, and the sections were cut to the desired thickness (3-μm thickness) using a microtome. The tissue sections were used for $A\beta_{1-40/42}$ and BDNF detection. The results were observed using microscopy.

The tissue sections were blocked in 10% normal serum with 1% BSA in Tris-buffered saline (TBS) for 2 h at room temperature. The sections were subsequently incubated with primary anti-$A\beta_{1-40/42}$ antibody or anti-BDNF antibody overnight at 4 °C. The sections were rinsed in TBS containing 0.025% Triton X-100 with gentle agitation and subsequently incubated in 0.3% distilled H_2O_2 in TBS for 15 min. The secondary antibody was applied to the slide at a dilution recommended by the manufacturer (in TBS with 1% BSA) and incubated for 1 h at room temperature. The labeling was visualized using 0.04% H_2O_2 and 0.05% 3,3′-diaminobenzidine. The results were calculated using ImageJ software 1.50i.

An AChE activity assay

The mouse brains were homogenized in a glass Teflon homogenizer containing 9 volumes of 0.9% saline solution and subsequently centrifuged at 800×*g* for 10 min at 4 °C. The resulting supernatant was collected and used in the AChE activity assay. AChE activity was detected using an AChE inhibitory activity assay kit according to the manufacturer's instructions.

A BuChE activity assay

Blood samples were collected from the mice in sodium heparin tubes and centrifuged at 4000×*g* for 10 min at 4 °C. Plasma was collected from the samples for use in a BuChE activity assay. BuChE activity was assessed using a BuChE inhibitory activity assay kit, according to the manufacturer's instructions.

Cell culture and treatments

We used stably co-transfected human neuroblastoma SH-SY5Y cells expressing APP-Swedish mutation and wild-type human APP (APPsw-SY5Y cells), as previously reported[31, 32]. In the absence of copper, the Aβ overexpression cell line exhibited no neurotoxicity in the culture process; the presence of copper triggered the toxicity of Aβ. In this AD cellular model, copper was used as a stimulator for Aβ-mediated neurotoxicity.

The cells were cultured in DMEM/F12 supplemented with 10% FBS, 1×10^5 U/L penicillin, and 100 mg/L streptomycin at 37 °C in a humidified, 5% CO_2 incubator. Subsequently, 200 μg/mL G418 was added into the medium to maintain the genotypically stable cell strains.

The cells were incubated with 10 μmol/L donepezil, 10 μmol/L rivastigmine, and 1, 3, and 10 μmol/L DL0410 for 2 h, followed by treatment with 200 μmol/L copper for 24 h. The cells and medium were subsequently collected to investigate the effects of DL0410.

A cell viability assay

After treatment, the medium was discarded and replaced with 100 μL of MTS (3-(4,5-dimethylthiazol-2-yl)-5-(3-carboxymethoxyphenyl)-2-(4-sulfophenyl)-2*H*-tetrazolium) solution according to the manufacturer's protocol. After a 2 h incubation at 37 °C, the absorbance at 490 nm was measured using a Spectra Max M5 microplate reader.

Mitochondrial membrane potential detection

Rh123 was used to detect changes in mitochondrial membrane potential (Δψm) in APPsw-SY5Y cells. After treatment as described above, APPsw-SY5Y cells were incubated with 10 μmol/L Rh123 for 30 min. The nucleic acid dye Hoechst 33342, used to identify cell nuclei, was added at a final concentration of 10 μmol/L at 10 min after the Rh123 incubation.

Fluorescent images and intensities were acquired and analyzed using a Cellomics Arrayscan V^{TI} HCS Reader (Thermo Fisher Scientific Cellomics, Pittsburgh, PA, USA). The Hoechst 33342- and Rh123-stained images were acquired using 386/23 nm excitation and 460/40 nm emission and 485/20 nm excitation and 535/50 nm emission wavelengths, respectively.

Western blot assay

Cells from the cerebral cortices of the mice were lysed in RIPA lysis buffer [50 mmol/L Tris-HCl (pH 7.4), 150 mmol/L NaCl, 20 mmol/L EDTA, 50 mmol/L sodium fluoride, 1 mmol/L sodium orthovanadate, 1% NP-40, 0.5% sodium deoxycholate, and 0.1% sodium dodecyl sulfate (SDS)]. The RIPA buffer was supplemented with complete protease inhibitor cocktail tablets (Roche Applied Science, Mannheim, Germany). The homogenates were centrifuged at 13 000×*g* for 20 min to obtain the desired supernatant.

Total protein concentrations were determined using the BCA method (CoWin Bioscience Co, Beijing, China). Equal amounts (30 μg) of protein samples were separated on 12% SDS-polyacrylamide gels and transferred to PVDF membranes (Millipore, MA, USA). The membranes were blocked with 5% BSA and 0.05% Tween-20 in TBS for 2 h at 37 °C, followed by overnight incubation with primary antibodies and incubation with HRP-conjugated secondary antibodies. Protein was detected using ChemiGlow Western Blotting Detection Reagents (CoWin Bioscience Co, Beijing, China). The results were quantified using Quantity One software (Bio-Rad, PA, USA).

An ELISA assay

The $A\beta_{1-42}$ in the culture medium was measured using a sensitive and specific ELISA assay according to the manufacturer's instructions (ExCell Biology, Shanghai, China). A total of 100 μL of sample was added to each well, followed by 50 μL of antibody. The solution was incubated at room temperature for 2 h. After several washes, an enzyme-conjugated secondary antibody (100 μL) was added to each well, and the ELISA plate was incubated at room temperature for 1 h. After additional washes, the substrate (100 μL) was added, followed by incubation at room temperature for 15 min. The reaction was stopped after adding stop buffer (100 μL); the absorbance at 490 nm was detected on a Spectra Max M5 microplate reader. A standard curve with known amounts of $A\beta_{1-42}$ was also generated. The $A\beta_{1-42}$ level was calculated according to the standard curve.

Statistical analysis

Statistical analyses were performed using SPSS software (version 16.0, SPSS Inc, Chicago, IL, USA). Group differences in the escape latency and search distance in the Morris water maze test were analyzed using two-way ANOVA with repeated measures. Other data were analyzed using one-way ANOVA followed by Tukey's *post hoc* test. All data are expressed as the mean±SEM. Statistical significance was defined as $P<0.05$ for all tests.

Results

The inhibitory effects of DL0410 on cholinesterase activity *in vitro*

The obtained IC_{50} values indicated that DL0410 exhibited AChE inhibitory activity similar to the non-competitive AChE inhibitor donepezil and had substantially greater inhibitory activity than rivastigmine. DL0410 also showed a potent BuChE inhibitory effect, with an IC_{50} value of 3.96 μmol/L. DL0410 exerted potent cholinesterase inhibitory effects *in vitro* in a concentration-dependent manner (Table 1).

The effect of DL0410 on the cell viability of APPsw-SY5Y cells subjected to copper

An AD cellular model comprising APPsw-SY5Y cells stimu-

Table 1. IC_{50} values of DL0410 as AChEI-BuChEI. Mean±SEM. *n*=3.

Sample number	AChEI (μmol/L)	BuChEI (μmol/L)	Raito of IC_{50} (BuChE/AChE)
DL0410	0.286±0.004	3.962±0.099	13.836
Rivastigmine	44.582±1.954	0.101±0.008	0.002
Donepezil	0.085±0.006	33.914±0.920	397.851
Iso-OMPA	–	2.373±0.102	–

lated with copper was employed to evaluate the neuroprotective effects of DL0410. As shown in Figure 2, treatment with 200 μmol/L of copper for 24 h resulted in 51.60% cell death (P<0.01 *vs* control). Pretreatment with various concentrations of DL0410 markedly increased cell viability (DL0410 1 μmol/L: 12.87% increase; DL0410 3 μmol/L: 18.20% increase; DL0410 10 μmol/L: 24.85% increase; P<0.01) compared with the Cu^{2+} induced APPsw-SY5Y cell damage model (Cu^{2+} model), and this increase was concentration-dependent. DL0410 showed better protection against Aβ-induced neurotoxicity than donepezil and rivastigmine at the same concentration (10 μmol/L).

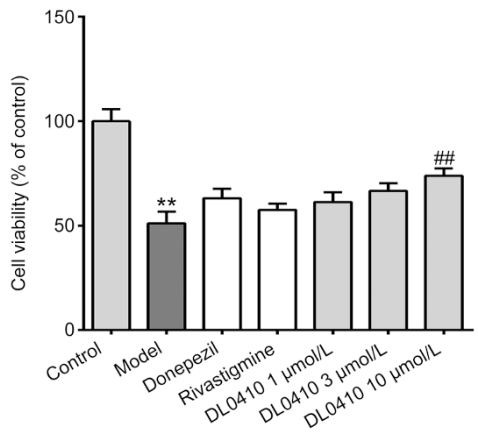

Figure 2. DL0410 improved the cell viability of APPsw-SY5Y cells subjected to copper. The results were obtained from 3 independent experiments, and the data are expressed as the mean±SEM. $^{**}P$<0.01 *vs* control. $^{\#\#}P$<0.01 *vs* the Cu^{2+} model.

The effect of DL0410 on $Aβ_{1-42}$-induced memory impairment

The effect of DL0410 on spatial memory was investigated via Morris water maze performance. MWM acquisition training tests were performed for five consecutive days, and the latency times were recorded. $Aβ_{1-42}$-treated mice showed more escape latency compared with vehicle-treated mice (P<0.01 *vs* sham, Figure 3A). The DL0410 treatment showed less latency than $Aβ_{1-42}$-treated mice (P<0.01 *vs* Aβ model, Figure 3A). We also observed that mice administered $Aβ_{1-42}$ had significantly longer latency time (P<0.001 *vs* sham, Figure 3B) and search distances (P<0.01 *vs* sham, Figure 3C) than vehicle-treated mice. The DL0410 treatment significantly decreased the latency (P<0.01 or P<0.001 *vs* Aβ model, Figure 3B) and search distance (P<0.01 *vs* Aβ model, Figure 3C). In the probe trial, compared with vehicle-treated mice, $Aβ_{1-42}$-treated mice showed reduced crossing numbers in the target quadrant (P<0.05 *vs* sham, Figure 3D). DL0410-treatment increased crossing numbers where the platform was located (P<0.05 *vs* Aβ model, Figure 3D). DL0410 had beneficial effects in attenuating spatial learning deficits in $Aβ_{1-42}$-treated mice.

The effect of DL0410 on memory impairment was also evaluated using passive avoidance tasks. Statistical analyses indicated that mice administered $Aβ_{1-42}$ showed significant memory deficits. The $Aβ_{1-42}$-treated mice had shorter latencies in entering the dark compartment (P<0.01 *vs* sham, Figure 3E) during the retention trial and made more errors during the acquisition trial (P<0.05 *vs* sham, Figure 3F). DL0410 treatments of 1, 3, and 9 mg/kg significantly prolonged the latency (P<0.01 *vs* Aβ model, Figure 3E) and decreased the error number (P<0.01 *vs* Aβ model, Figure 3F), indicating that DL0410 remarkably protected mice from $Aβ_{1-42}$-induced memory deficits in a dose-dependent manner at dosages of 1 to 9 mg/kg.

The effects of DL0410 on Aβ levels in an $Aβ_{1-42}$-induced amnesia mouse model and on APPsw-SY5Y cells

The effects of DL0410 on Aβ levels in the $Aβ_{1-42}$-induced amnesia mouse model were evaluated. Previously, we designed this test to detect the Aβ level in the cortex region to ensure that the injected exogenous Aβ would be distributed through the brain. Immunohistochemical assays showed a large number of $Aβ_{1-40/1-42}$ deposits in the cortices of $Aβ_{1-42}$-treated mice (Figure 4Ab), but no detectable $Aβ_{1-40/42}$ deposits were observed in sham-treated mice (Figure 4Aa). Compared with $Aβ_{1-42}$-treated mice, the DL0410 treatment reduced the areas of Aβ deposits in the cortices in a dose-dependent manner (Figure 4Ad, 4Ae, 4Af). Western blot results revealed that 9 mg/kg DL0410 significantly decreased β-APP protein levels in the cerebral cortices of $Aβ_{1-42}$-treated mice (P<0.05 *vs* Aβ model, Figure 4B).

APPsw-SY5Y cells were used to examine the effects of DL0410 on Aβ levels *in vitro*. An ELISA assay was applied to detect extracellular $Aβ_{1-42}$ levels. As shown in Figure 4C, treatment with copper significantly increased $Aβ_{1-42}$ production compared with untreated controls (P<0.05 *vs* control). Pretreatment with 10 μmol/L DL0410 markedly reduced the levels of extracellular $Aβ_{1-42}$ by 19.05% (P<0.05 *vs* Cu^{2+} model), and DL0410 decreased copper-stimulated $Aβ_{1-42}$ production in a concentration-dependent manner.

The effects of DL0410 on CREB and BDNF expression in an $Aβ_{1-42}$-induced amnesia mouse model

CREB phosphorylation was detected using a Western blot assay, and hippocampal BDNF levels were assessed through immunohistochemistry. As shown in Figure 5, the Western blot results revealed that the DL0410 treatment significantly increased the ratio of p-CREB/CREB in the cerebral cortices of $Aβ_{1-42}$-treated mice (P<0.05 *vs* Aβ model, Figure 5A). In addition, DL0410 increased the number of BDNF-positive neurons

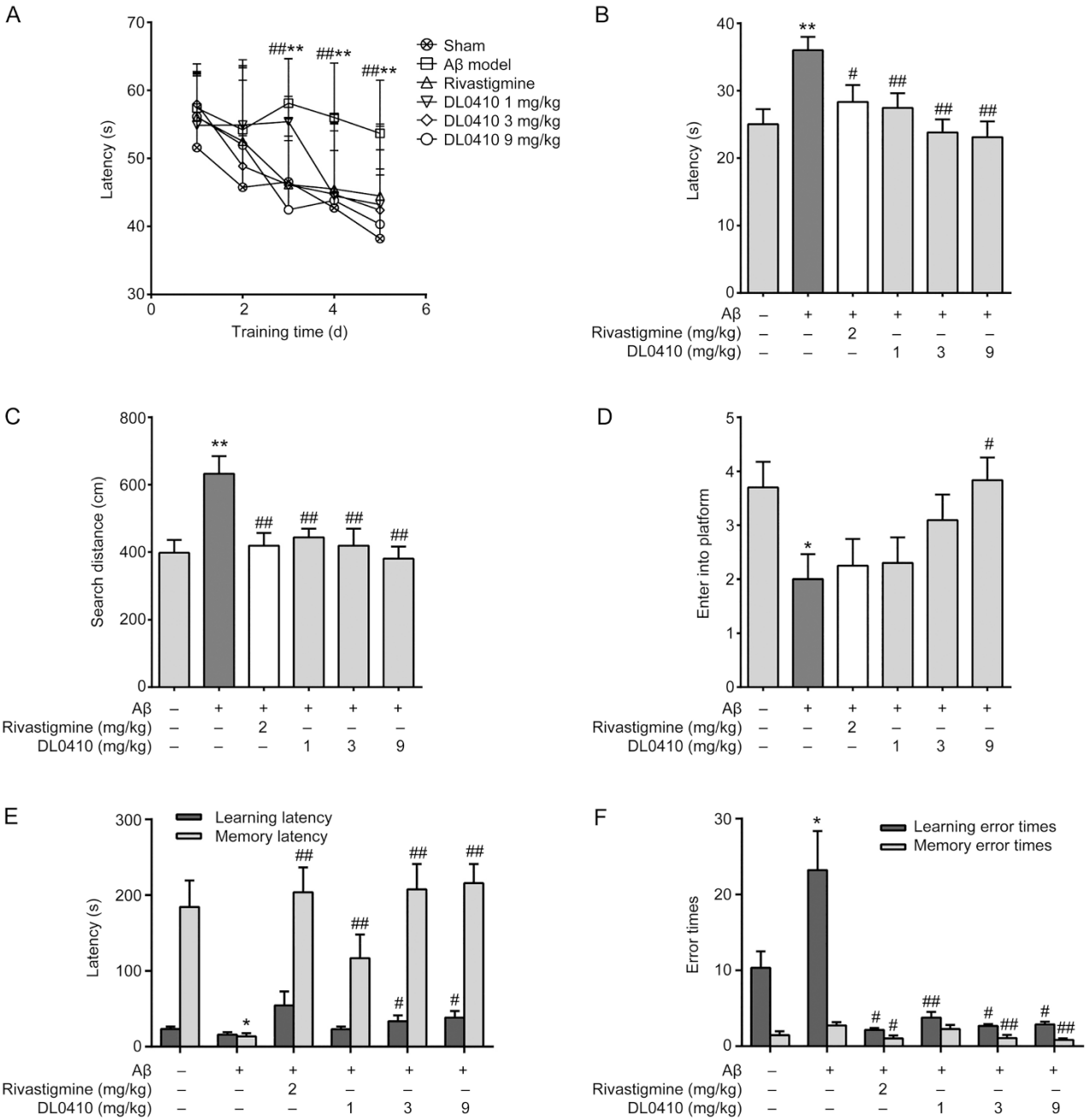

Figure 3. The effects of DL0410 on learning and memory capabilities in an $A\beta_{1-42}$-induced amnesia mouse model. The data are expressed as the mean±SEM. n=15. (A) DL0410 shortened the latency time to the hidden platform during Morris water maze performance. (B) DL0410 decreased the latency to the platform during Morris water maze performance in the 5th training day in another independent experiment. (C) DL0410 decreased the search distance to the platform in the Morris water maze. (D) DL0410 increased crossing numbers in the target quadrant in the probe trial. (E) DL0410 prolonged the latency to enter the dark compartment in the passive avoidance test. (F) DL0410 decreased the number of errors in the passive avoidance test. $^{*}P$<0.05, $^{**}P$<0.01 *vs* sham. $^{\#}P$<0.05, $^{\#\#}P$<0.01 *vs* the Aβ model.

in the cortices of $A\beta_{1-42}$-treated mice (Figure 5B).

The effects of DL0410 on cholinesterase activity in an $A\beta_{1-42}$-induced amnesia mouse model

The effects of DL0410 on brain AChE and plasma BuChE activity were detected. As shown in Figure 6A, AChE activity in the $A\beta_{1-42}$-treated group was significantly increased (P<0.05 *vs* sham). Lower AChE activity was observed in the rivastigmine- and DL0410-treated groups compared with the $A\beta_{1-42}$-treated group, but these differences were not statistically significant. $A\beta_{1-42}$-treated mice also showed significantly increased BuChE activity (P<0.05 *vs* sham, Figure 6B), whereas rivastigmine and the DL0410 treatments decreased BuChE activity (P<0.01 *vs* Aβ model, P<0.001 *vs* Aβ model, Figure 6B).

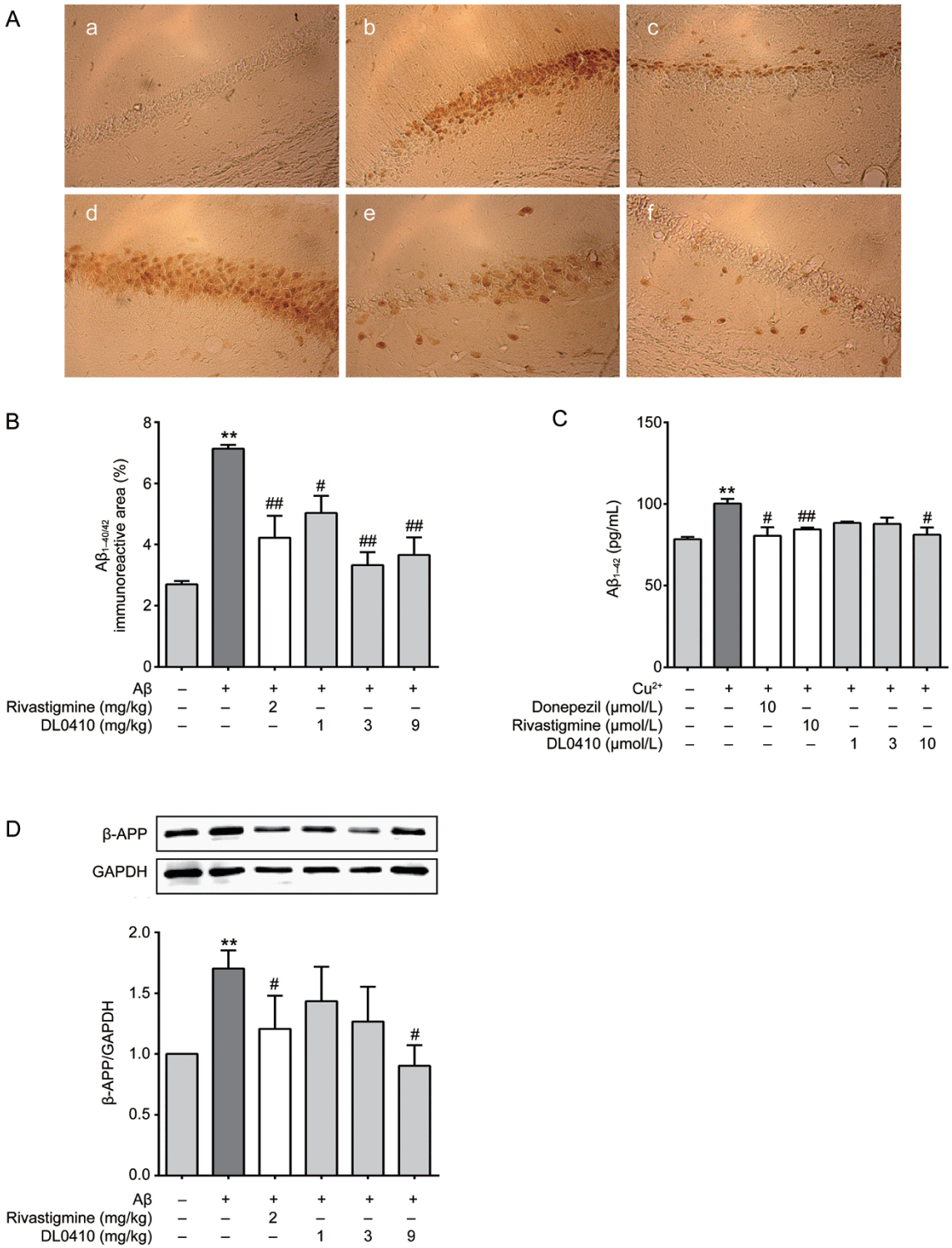

Figure 4. DL0410 inhibited the level of Aβ in the $Aβ_{1-42}$-induced amnesia mouse model and in APPsw-SY5Y cells. (A) DL0410 decreased $Aβ_{1-40/42}$ deposits in mouse cerebral cortices: (a) sham group, (b) Aβ group, (c) Aβ+rivastigmine (2 mg/kg) group, (d) Aβ+DL0410 (1 mg/kg) group, (e) Aβ+DL0410 (3 mg/kg) group, and (f) Aβ+DL0410 (9 mg/kg) group. (B) The percentage of $Aβ_{1-40/42}$ positive cells in the cortex. The data are expressed as the mean±SEM. n=5. $^{**}P$<0.01 *vs* sham. $^{\#}P$<0.05, $^{\#\#}P$<0.01 *vs* model. (C) The effects of DL0410 on $Aβ_{1-42}$ production *in vitro*. APPsw-SY5Y cells were incubated with Cu^{2+} 200 μmol/L for 24 h to induce $Aβ_{1-42}$ production; the amounts of $Aβ_{1-42}$ in the culture media were measured through an ELISA assay. The results were obtained from 3 independent experiments, and the data are expressed as the mean±SEM. $^{**}P$<0.01 *vs* control. $^{\#}P$<0.05, $^{\#\#}P$<0.01 *vs* the Cu^{2+} model. (D) DL0410 suppressed β-APP expression in the $Aβ_{1-42}$-induced amnesia mouse model. The expression of β-APP in the cerebral cortex was determined using the Western blot assay. The data are expressed as the mean±SEM. n=5. $^{**}P$<0.01 *vs* sham. $^{\#}P$<0.05 *vs* the Aβ model.

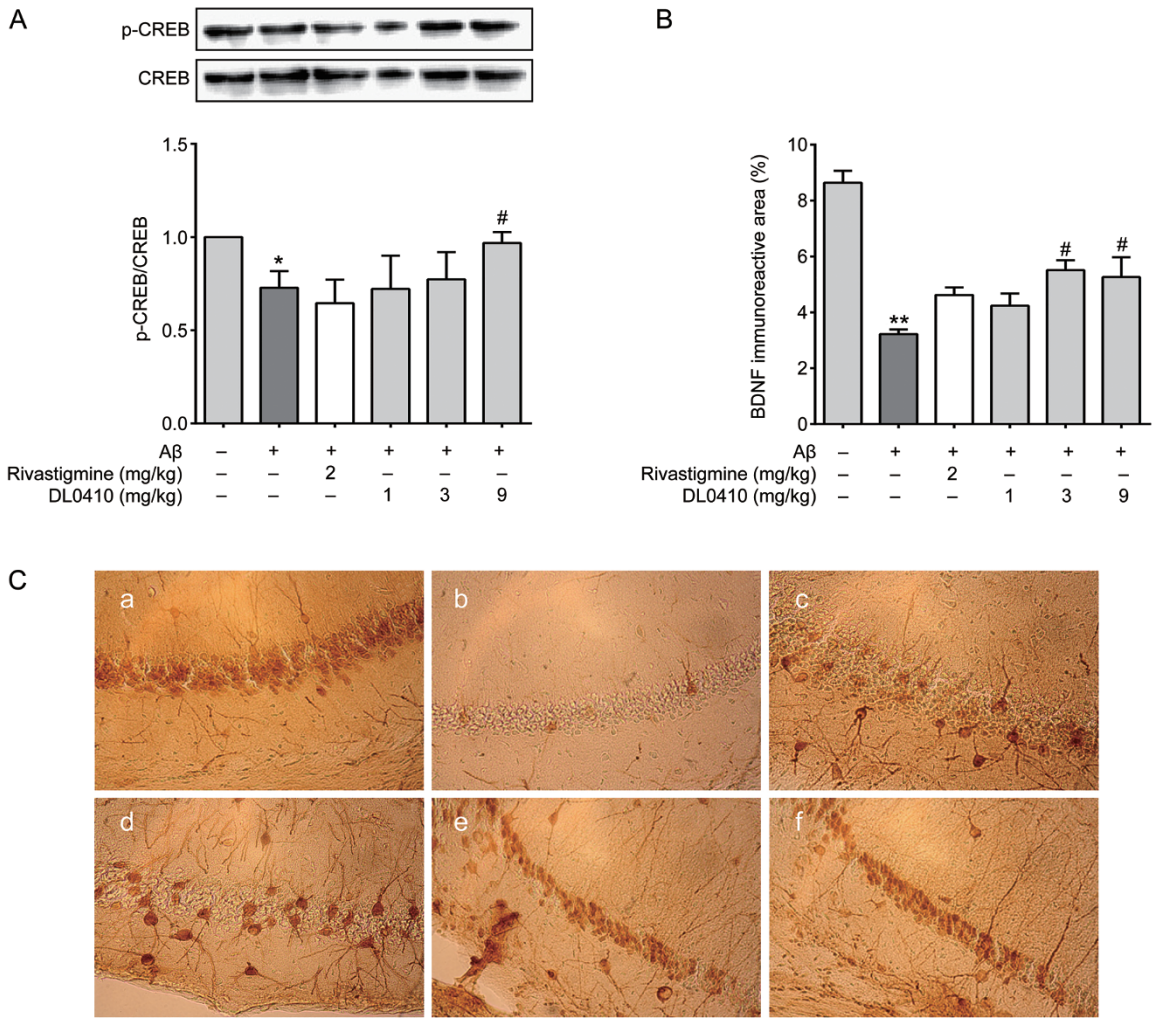

Figure 5. The effects of DL0410 on CREB and BDNF expression in an $A\beta_{1-42}$-induced amnesia mouse model. (A) The effect of DL0410 on p-CREB and total-CREB expression in the cerebral cortices of $A\beta_{1-42}$-treated mice. The data are expressed as the mean±SEM. n=5. $^{*}P$<0.05 *vs* sham. $^{\#}P$<0.05 *vs* the Aβ model. (B) The percentage of positive BDNF cells in the cortex. (C) DL0410-normalized, $A\beta_{1-42}$-induced decreases in BDNF levels in mouse cortices: (a) sham group, (b) Aβ group, (c) Aβ+rivastigmine (2 mg/kg) group, (d) Aβ+DL0410 (1 mg/kg) group, (e) Aβ+DL0410 (3 mg/kg) group, and (f) Aβ+DL0410 (9 mg/kg) group. The data are expressed as the mean±SEM. n=5. $^{*}P$<0.05, $^{**}P$<0.01 *vs* sham. $^{\#}P$<0.05 *vs* the Aβ model.

The effect of DL0410 on mitochondrial function in copper-treated APPsw-SY5Y cells

The protective effect of DL0410 on the mitochondrial function in copper-treated APPsw-SY5Y cells was investigated using Rh123 fluorescent dye, and the Δψm was monitored as the fluorescence intensity of Rh123. When the cells were exposed to 200 μmol/L copper for 24 h, the mitochondrial membranes were depolarized, and the fluorescence intensity increased by 211.50% (P<0.01 *vs* control). Pretreatment with DL0410 reduced the fluorescence intensity in a concentration-dependent manner (P<0.05 *vs* Cu^{2+} model, Figure 7B), suggesting that DL0410 protects APPsw-SY5Y cells by reversing copper-induced Δψm loss.

The effects of DL0410 on the apoptosis-related Akt/JNK signaling pathway in copper-treated APPsw-SY5Y cells

The effects of DL0410 on the Akt/JNK pathway were also assessed using a Western blot assay. Copper-treated APPsw-SY5Y cells showed a significantly increased ratio of p-JNK/JNK (P<0.05 *vs* control, Figure 8A) and a remarkably decreased ratio of p-Akt/Akt (P<0.01 *vs* control, Figure 8B). In contrast, the DL0410 treatment decreased the phosphorylation of JNK and increased the phosphorylation of Akt (P<0.05 *vs* Cu^{2+} model, Figure 8). These data indicated that DL0410 might attenuate cell apoptosis through the regulation of the Akt/JNK pathway.

Discussion

The results of the present study demonstrated that DL0410 improved learning and memory dysfunction in $A\beta_{1-42}$-treated mice and reduced mitochondria-mediated APPsw-SY5Y cell apoptosis. The mechanism of these beneficial effects might reflect cholinesterase inhibition, Aβ production inhibition and CREB/BDNF pathway and the Akt/JNK pathway regulation.

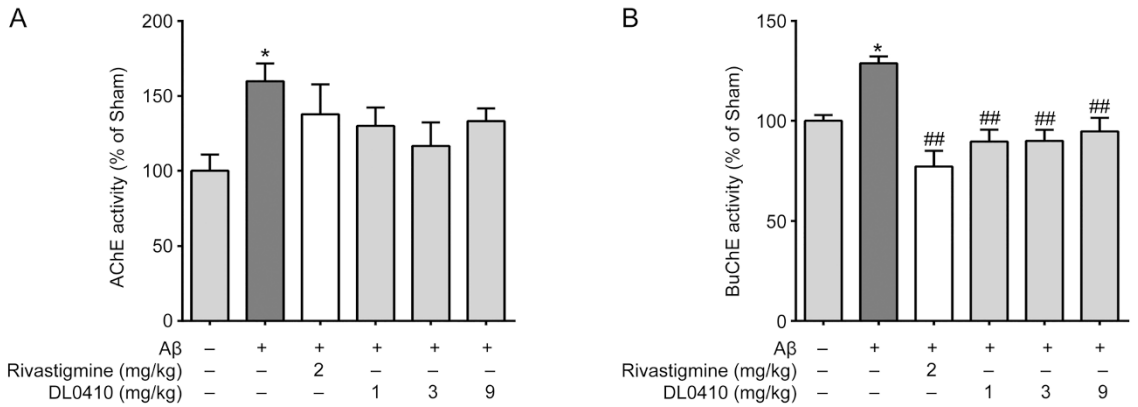

Figure 6. The effects of DL0410 on cholinesterase activity in an $A\beta_{1-42}$-induced amnesia mouse model. (A) Effects of DL0410 on brain AChE activity in the $A\beta_{1-42}$-induced amnesia mouse model. The data are expressed as the mean±SEM. n=5. $^{*}P$<0.05 *vs* sham. (B) DL0410 decreased plasma BuChE activity in the $A\beta_{1-42}$-induced amnesia mouse model. The data are expressed as the mean±SEM. n=5. $^{*}P$<0.05 *vs* sham. $^{\#\#}P$<0.01 *vs* the Aβ model.

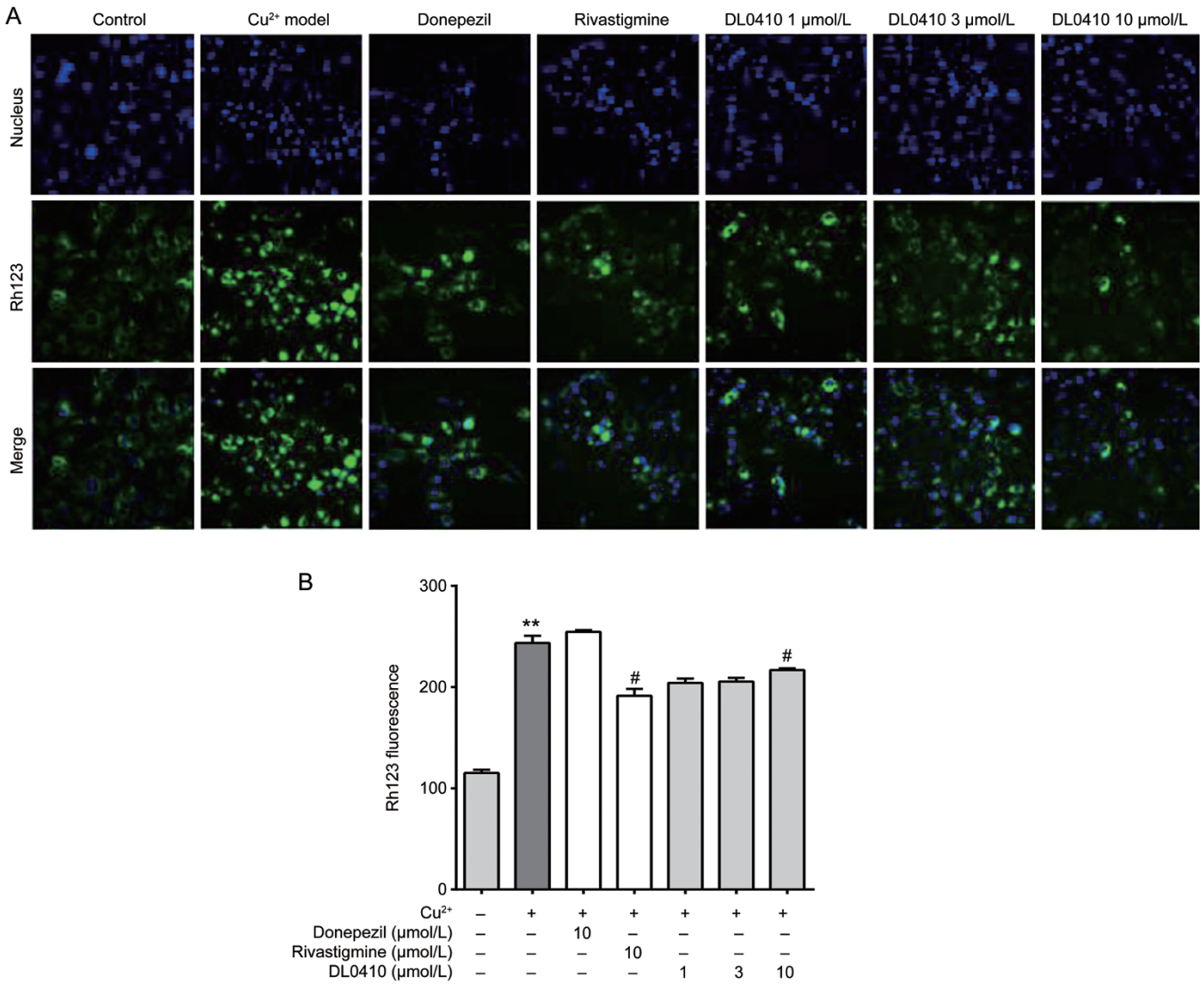

Figure 7. The effect of DL0410 on mitochondrial membrane potential in APPsw-SY5Y cells exposed to copper. (A) Representative photographs of Rh123 staining in different groups. (B) Quantitative analysis of Rh123 fluorescence intensity among the groups. The results were obtained from 3 independent experiments, and the data are expressed as the mean±SEM. $^{**}P$<0.01 *vs* control. $^{\#}P$<0.05 *vs* the Cu^{2+} model.

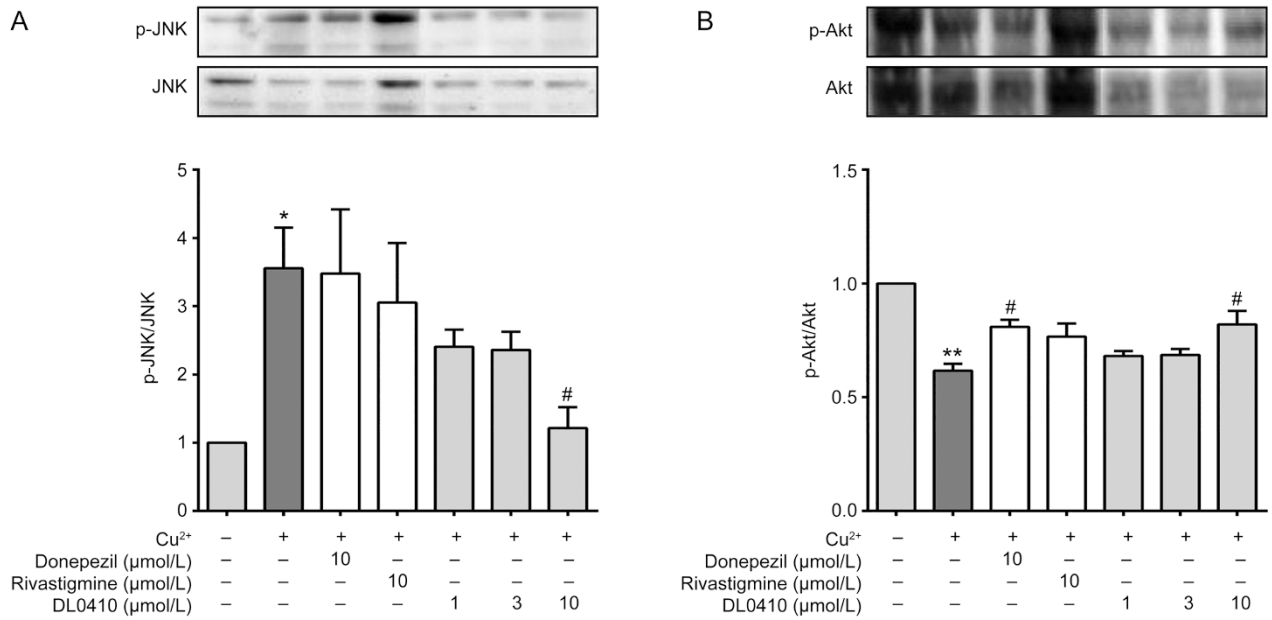

Figure 8. DL0410 attenuated cell apoptosis through the regulation of the Akt/JNK pathway. (A) The effects of DL0410 on p-JNK and total JNK expression in copper-treated APPsw-SY5Y cells. (B) The effects of DL0410 on p-Akt and total Akt expression in copper-treated APPsw-SY5Y cells. The results were obtained from 3 independent experiments, and the data are expressed as the mean±SEM. $^{*}P<0.05$, $^{**}P<0.01$ *vs* control. $^{\#}P<0.05$ *vs* the Cu^{2+} model.

The "amyloid hypothesis" suggests that the abnormal deposition of amyloid-β peptide in the brain plays a key role in AD pathogenesis, as the extracellular Aβ accumulation is a pathological hallmark of AD[33, 34]. Aβ has neurotoxicity effects on cholinergic neurons and the learning function[35–38]. In addition, cognitive function improvement is the primary goal of AD clinical treatment, and cholinesterase inhibitors have been broadly established as a first-line AD symptomatic therapy[39]. *In vitro* data demonstrated that DL0410 has potent AChE and BuChE inhibitory effects compared with clinically approved medications, such as donepezil and rivastigmine, and the DL0410 treatment decreased extracellular $A\beta_{1-42}$ levels and increased cell viability in copper-induced toxicity in APPsw-SY5Y cell lines. To investigate the neuroprotective effect of DL0410 on cognitive impairment and cholinesterase deficits *in vivo*, we established an acute intracerebroventricular injection $A\beta_{1-42}$ mouse model and copper-treated APPsw-SY5Y cell model[31, 32]. *In vivo* data suggested that the intracerebroventricular infusion of $A\beta_{1-42}$ resulted in significant learning and memory impairment, and DL0410 significantly improved behavioral performance in a dose-dependent manner. Furthermore, DL0410 exerted an inhibitory effect on AChE and BuChE activities. To evaluate whether the behavioral improvement observed in the DL0410-treated mice was correlated with changes in Aβ metabolism, we analyzed the presence of Aβ deposits and β-APP protein levels in the brains of $A\beta_{1-42}$-treated mice. We showed that the DL0410 treatment attenuated $A\beta_{1-42}$-induced Aβ overproduction in the mouse brain. The results from *in vivo* and *in vitro* studies indicated that the regulation of Aβ production represents a potential neuroprotective mechanism of DL0410 in AD therapy.

CREB is a widely expressed nuclear transcription factor that plays a critical role in learning and memory. The expression of phosphorylated CREB in transgenic mice and disease patients is reduced, leading to a reduction in the BDNF level. Hence, the CREB/BDNF signaling pathway might act as a key modulator in the pathophysiology of AD[40–42]. To further examine the molecular mechanism underlying the improvement of AD impairment through DL0410, we assessed the effects of DL0410 on the phosphorylation of CREB and the expression of BDNF protein in the brains of $A\beta_{1-42}$-treated mice. According to the present study, DL0410 (9 mg/kg) significantly increased the phosphorylation of CREB in the cerebral cortices of $A\beta_{1-42}$-treated mice. DL0410 increased the number of BDNF-positive neurons in the mice cortices. This *in vivo* mechanism study indicated that the protective effect of DL0410 might be associated with the up-regulation of the above signaling pathway.

Mitochondria play a critical role in neuronal energy supply and synaptic plasticity[43–45]. Many studies have suggested that mitochondrial dysfunction is a common feature in AD neurons[46]. It has also been reported that mitochondria-derived reactive oxygen species enhance amyloidogenic amyloid precursor protein processing, whereas Aβ leads to mitochondrial functional impairment[47]. In the present *in vitro* study, when cells were treated with copper for 24 h, the mitochondrial membranes were depolarized, and DL0410 significantly alleviated mitochondrial dysfunction through improvements in mitochondrial membrane potential.

We further investigated the molecular components involved in the mitochondria- mediated apoptosis pathway. Based on

in vivo experiments, DL0410 increased CREB activity in the brains of $A\beta_{1-42}$-treated mice. Studies have confirmed that the activation of CREB is positively regulated through Akt[48–52]. Akt plays important roles in preventing cell apoptosis[53]. The activity of JNK is negatively regulated through Akt, whereas JNK activation is involved in the mitochondria-mediated apoptosis pathway[42, 43]. We observed that APPsw-SY5Y cells exposed to copper exhibited increased levels of p-JNK and decreased levels of p-Akt. DL0410 significantly increased the phosphorylation of Akt and suppressed the phosphorylation of JNK. The results of the present study suggested that DL0410 attenuates Aβ-induced (stimulated through copper) apoptosis via the regulation of the Akt/JNK pathway.

In conclusion, the present study examined the therapeutic potential of DL0410 in Aβ-induced cognitive impairment and neuronal damage. The results demonstrated that DL0410 exhibited potent inhibitory effects on cholinesterase, improved learning and memory dysfunction in rodents, and exhibited neuroprotective effects both *in vitro* and *in vivo*. The Akt/JNK pathway was involved in the neuroprotective effects of DL0410. These results indicated that DL0410 is a potential pharmaceutical candidate for AD therapy.

Acknowledgements

This research work was financially supported by grants from the Research Special Fund for the Public Welfare Industry of Health (No 200802041), the National Great Science and Technology Projects (No 2013ZX09402203 and 2014ZX09507003-002), and the International Collaboration Project (No 2011DFR31240). The abstract of this manuscript had previously been submitted to the 17th World Congress of Basic & Clinical Pharmacology[54].

Author contribution

Guan-hua DU and Ai-lin LIU designed the experiment and revised the manuscript; Dan ZHOU, Wei ZHOU, Jun-ke SONG, Zhang-ying FENG, and Ran-yao YANG performed the experiments; Jun-ke SONG helped to edit several figures and analyse data; Song WU and Lin WANG supplied the DL0410 compound; Dan ZHOU and Wei ZHOU analyzed the data.

References

1 Alzheimer's Association. 2012 Alzheimer's disease facts and figures. Alzheimers Dement 2012; 8: 131–68.
2 Jack CR Jr, Albert MS, Knopman DS, McKhann GM, Sperling RA, Carrillo MC, *et al*. Introduction to the recommendations from the National Institute on Aging-Alzheimer's Association workgroups on diagnostic guidelines for Alzheimer's disease. Alzheimers Dement 2011; 7: 257–62.
3 Francis PT, Ramírez MJ, Lai MK. Neurochemical basis for symptomatic treatment of Alzheimer's disease. Neuropharmacology 2010; 59: 221–9.
4 Klinkenberg I, Blokland A. The validity of scopolamine as a pharmacological model for cognitive impairment: a review of animal behavioral studies. Neurosci Biobehav Rev 2010; 34: 1307–50.
5 Darvesh S, Hopkins DA, Geula C. Neurobiology of butyrylcholinesterase. Nat Rev Neurosci 2003; 4: 131–8.
6 Greig NH, Utsuki T, Ingram DK, Wang Y, Pepeu G, Scali C, *et al*. Selective butyrylcholinesterase inhibition elevates brain acetylcholine, augments learning and lowers Alzheimer beta-amyloid peptide in rodent. Proc Natl Acad Sci U S A 2005; 102: 17213–8.
7 Giacobini E. Cholinesterase inhibitors: new roles and therapeutic alternatives. Pharmacol Res 2004; 50: 433–40.
8 Bourne Y, Taylor P, Radić Z, Marchot P. Structural insights into ligand interactions at the acetylcholinesterase peripheral anionic site. EMBO J 2003; 22: 1–12.
9 Galdeano C, Viayna E, Arroyo P, Bidon-Chanal A, Blas JR, Muñoz-Torrero D, *et al*. Structural determinants of the multifunctional profile of dual binding site acetylcholinesterase inhibitors as anti-Alzheimer agents. Curr Pharm Des 2010; 16: 2818–36.
10 Rees T, Hammond PI, Soreq H, Younkin S, Brimijoin S. Acetylcholinesterase promotes beta-amyloid plaques in cerebral cortex. Neurobiol Aging 2003; 24: 777–87.
11 Darvesh S, Cash MK, Reid GA, Martin E, Mitnitski A, Geula C. Butyrylcholinesterase is associated with β-amyloid plaques in the transgenic APPSWE/PSEN1dE9 mouse model of Alzheimer disease. J Neuropathol Exp Neurol 2012; 71: 2–14.
12 Bailey JA, Lahiri DK. A novel effect of rivastigmine on pre-synaptic proteins and neuronal viability in a neurodegeneration model of fetal rat primary cortical cultures and its implication in Alzheimer's disease. J Neurochem 2010; 112: 843–53.
13 O'Brien RJ, Wong PC. Amyloid precursor protein processing and Alzheimer's disease. Annu Rev Neurosci 2011; 34: 185–204.
14 Sipos E, Kurunczi A, Kasza A, Horváth J, Felszeghy K, Laroche S, *et al*. Beta-amyloid pathology in the entorhinal cortex of rats induces memory deficits: implications for Alzheimer's disease. Neuroscience 2007; 147: 28–36.
15 Zhu X, Chen C, Ye D, Guan D, Ye L, Jin J, *et al*. Diammonium glycyrrhizinate upregulates PGC-1α and protects against $A\beta_{1-42}$-induced neurotoxicity. PLoS One 2012; 7: e35823.
16 Liu RT, Zou LB, Lü QJ. Liquiritigenin inhibits $A\beta_{25-35}$-induced neurotoxicity and secretion of $A\beta_{1-40}$ in rat hippocampal neurons. Acta Pharmacol Sin 2009; 30: 899–906.
17 Park H, Oh MS. Houttuyniae Herba protects rat primary cortical cells from $A\beta_{25-35}$-induced neurotoxicity via regulation of calcium influx and mitochondria-mediated apoptosis. Hum Exp Toxicol 2012; 31: 698–709.
18 Quintanilla RA, Dolan PJ, Jin YN, Johnson GV. Truncated tau and Aβ cooperatively impair mitochondria in primary neurons. Neurobiol Aging 2012; 33: 619.e25–35.
19 Clevers H, Nusse R. WNT/β-catenin signaling and disease. Cell 2012; 149: 1192–205.
20 Oddo S. The role of mTOR signal pathway in Alzheimer disease. Front Biosci 2014; 4: 941–52.
21 Heras-Sandoval D, Perez-Rojas JM, Hernandez-Damian J, Pedraza-Chaverri J. The role of PI3K/AKT/mTOR pathway in the modulation of autophagy and the clearance of protein aggregates in neurodegeneration. Cell Signal 2014; 26: 2694–701.
22 Ma T, Chen Y, Vingtdeux V, Zhao H, Viollet B, Marambaud P, *et al*. Inhibition of AMP-activated protein kinase signaling alleviates impairments in hippocampal synaptic plasticity induced by amyloid. J Neurosci 2014; 34: 12230–8.
23 Bonda DJ, Lee HG, Camins A, Pallàs M, Casadesus G, Smith MA, *et al*. The sirtuin pathway in ageing and Alzheimer disease: mechanistic and therapeutic considerations. Lancet Neurol 2011; 10: 275–9.
24 Fang J, Yang RY, Gao L, Zhou D, Yang S, Liu AL, *et al*. Predictions of BuChE inhibitors using support vector machine and naive bayesian classification techniques in drug discovery. J Chem Inf Model 2013;

53: 3009–20.
25 Yang RY, Zhao G, Wang DM, Pang XC, Wang SB, Fang JS, *et al*. DL0410 can reverse cognitive impairment, synaptic loss and reduce plaque load in APP/PS1 transgenic mice. Pharmacol Biochem Behav 2015; 139: 15–26.
26 Ellman GL, Courtney KD, Andres V Jr, Feather-Stone RM. A new and rapid colorimetric determination of acetylcholinesterase activity. Biochem Pharmacol 1961; 7: 88–95.
27 Walker DG, Lue LF, Reid R, Sabbagh MN. P2–273: chronic rivastigmine administration reduces beta-amyloid levels in transgenic mouse model for Alzheimer's disease. Alzheimer Dementia 2008; 4: T482.
28 Song L, Che W, Wang MW, Murakami Y, Matsumoto K. Impairment of the spatial learning and memory induced by learned helplessness and chronic mild stress. Pharmacol Biochem Behav 2006; 83: 186–93.
29 Lu J, Wu DM, Zheng YL, Sun DX, Hu B, Shan Q, *et al*. Trace amounts of copper exacerbate beta amyloid-induced neurotoxicity in the cholesterol-fed mice through TNF-mediated inflammatory pathway. Brain Behav Immun 2009; 23: 193–203.
30 Shanks M, Kivipelto M, Bullock R, Lane R. Cholinesterase inhibition: is there evidence for disease-modifying effects? Curr Med Res Opin 2009; 25: 2439–46.
31 Liu R, Wu CX, Zhou D, Yang F, Tian S, Zhang L, *et al*. Pinocembrin protects against beta-amyloid-induced toxicity in neurons through inhibiting receptor for advanced glycation end products (RAGE)-independent signaling pathways and regulating mitochondrion-mediated apoptosis. BMC Med 2012; 10: 105.
32 Singh SK, Sinha P, Mishra L, Srikrishna S. Neuroprotective role of a novel copper chelator against $A\beta_{42}$ induced neurotoxicity. Int J Alzheimers Dis 2013; 567128.
33 Glenner GG, Wong CW. Alzheimer's disease and Down's syndrome: sharing of a unique cerebrovascular amyloid fibril protein. Biochem Biophys Res Commun 1984; 122: 1131–5.
34 Reitz C. Alzheimer's disease and the amyloid cascade hypothesis: a critical review. Int J Alzheimers Dis 2012; 2012: 369808.
35 Nitta A, Itoh A, Hasegawa T, Nabeshima T. β-Amyloid protein-induced Alzheimer's disease animal model. Neurosci Lett 1994; 170: 63–6.
36 Kar S, Issa AM, Seto D, Auld DS, Collier B, Quirion R. Amyloid β-peptide inhibits high-affinity choline uptake and acetylcholine release in rat hippocampal slices. J Neurochem 1998; 70: 2179–87.
37 Nakdook W, Khongsombat O, Taepavarapruk P, Taepavarapruk N, Ingkaninan K. The effects of *Tabernaemontana divaricata* root extract on amyloid beta-peptide 25–35 peptides induced cognitive deficits in mice. J Ethnopharmacol 2010; 130: 122–6.
38 Rovira C, Arbez N, Mariani J. $A\beta_{25-35}$ and $A\beta_{1-40}$ act on different calcium channels in CA1 hippocampal neurons. Biochem Biophys Res Commun 2002; 296: 1317–21.
39 Sipos E, Kurunczi A, Kasza A, Horváth J, Felszeghy K, Laroche S, *et al*. Beta-amyloid pathology in the entorhinal cortex of rats induces memory deficits: implications for Alzheimer's disease. Neuroscience 2007; 147: 28–36.
40 Warburton EC, Glover CP, Massey PV, Wan H, Johnson B, Bienemann A, *et al*. cAMP responsive element-binding protein phosphorylation is necessary for perirhinal long-term potentiation and recognition memory. J Neurosci 2005; 25: 6296–303.
41 Verma SK, Raheja G, Gill KD. Role of muscarinic signal transduction and CREB phosphorylation in dichlorvos-induced memory deficits in rats: an acetylcholine independent mechanism. Toxicology 2009; 256: 175–82.
42 Moncada D, Viola H. Phosphorylation state of CREB in the rat hippocampus: a molecular switch between spatial novelty and spatial familiarity. Neurobiol Learn Mem 2006; 86: 9–18.
43 Lee J, Giordano S, Zhang J. Autophagy, mitochondria and oxidative stress: cross-talk and redox signalling. Biochem J 2012; 441: 523–40.
44 Su K, Bourdette D, Forte M. Genetic inactivation of mitochondria targeted redox enzyme p66ShcA preserves neuronal viability and mitochondrial integrity in response to oxidative challenges. Front Physiol 2012; 3: 285.
45 De Vos KJ, Grierson AJ, Ackerley S, Miller CC. Role of axonal transport in neurodegenerative diseases. Annu Rev Neurosci 2008; 31: 151–73.
46 Silva-Alvarez C, Arrázola MS, Godoy JA, Ordenes D, Inestrosa NC. Canonical Wnt signaling protects hippocampal neurons from Aβ oligomers: role of non-canonical Wnt-5a/Ca^{2+} in mitochondrial dynamics. Front Cell Neurosci 2013; 7: 97.
47 Leuner K, Schütt T, Kurz C, Eckert SH, Schiller C, Occhipinti A, *et al*. Mitochondrion-derived reactive oxygen species lead to enhanced amyloid beta formation. Antioxid Redox Signal 2012; 16: 1421–33.
48 De Butte-Smith M, Zukin RS, Etgen AM. Effects of global ischemia and estradiol pretreatment on phosphorylation of Akt, CREB and STAT3 in hippocampal CA1 of young and middle-aged female rats. Brain Res 2012; 1471: 118–28.
49 Li XY, Zhan XR, Liu XM, Wang XC. CREB is a regulatory target for the protein kinase Akt/PKB in the differentiation of pancreatic ductal cells into islet β-cells mediated by hepatocyte growth factor. Biochem Biophys Res Commun 2011; 404: 711–6.
50 Hers I, Vincent EE, Tavaré JM. Akt signalling in health and disease. Cell Signal 2011; 23: 1515–27.
51 Song G, Ouyang G, Bao S. The activation of Akt/PKB signaling pathway and cell survival. J Cell Mol Med 2005; 9: 59–71.
52 Humar M, Loop T, Schmidt R, Hoetzel A, Roesslein M, Andriopoulos N, *et al*. The mitogen-activated protein kinase p38 regulates activator protein 1 by direct phosphorylation of c-Jun. Int J Biochem Cell Biol 2007; 39: 2278–88.
53 Gao N, Budhraja A, Cheng S, Liu EH, Chen J, Yang Z, *et al*. Phenethyl isothiocyanate exhibits antileukemic activity *in vitro* and *in vivo* by inactivation of Akt and activation of JNK pathways. Cell Death Dis 2011; 2: e140.
54 Liu AL, Zhou D, Yang RY, Liu R, Du GH. DL0410, a novel anti-alzheimer's disease candidate, protects neuron against Aβ-induced cell damage via α7nAChR medicated intracellular Akt/JNK signaling pathway. Basic Clin Pharmacol Toxicol 2014; 115: 112.